



# Processing and characterization of novel *Himalayacalamus falconeri* fiber reinforced biodegradable composites

Mayank Pokhriyal<sup>1,2</sup> · Pawan Kumar Rakesh<sup>1</sup>

Received: 5 February 2023 / Revised: 7 April 2023 / Accepted: 10 April 2023 / Published online: 28 April 2023  
© The Author(s), under exclusive licence to Springer-Verlag GmbH Germany, part of Springer Nature 2023

## Abstract

In the present experimental investigation, novel *Himalayacalamus falconeri* fiber reinforced polylactic acid biocomposites were developed via direct injection molding. Standard test procedures were used to evaluate the mechanical, thermal, microstructural, and water absorption properties of the developed biocomposites as a function of fiber concentration (5–20%) and alkali treatment (5% w/v NaOH solution). It was observed that the tensile, flexural, and impact strength of all developed biocomposites were gradually enhanced with the addition of fiber concentration up to 15 wt.% and thereafter start decreasing with increasing fiber concentration up to 20%. Alkali-treated biocomposite with 15 wt.% fiber content (PLA/THF-15) exhibited the highest tensile strength (44.59 MPa ± 1.55 MPa) and flexural strength (75.68 MPa ± 0.88 MPa). Untreated biocomposite (PLA/UHF-15) showed a maximum impact strength of 41.61 J/m. Meanwhile, the fractured surfaces from mechanical testing were examined using a scanning electron microscope to identify the causes of failure in the developed biocomposites. Alkali-treated biocomposite with 20 wt.% fiber content (PLA/THF-20) exhibited the highest hardness value of 90.66 HD, while untreated biocomposite with 20 wt.% fiber content (PL/UHF-20) exhibited the maximum water absorption rate (2.60%) and soil degradation rate (2.18%). The Vicat softening temperature (VST) and heat deflection temperature (HDT) were found to be 56.7 °C for PL/THF-20 and 57.55 °C for PLA/THF-15, respectively. It can be concluded from this present investigation that short *Himalayacalamus falconeri* fiber can be used as reinforcement in PLA-based matrix to make entirely biodegradable green composites that can replace petroleum-based synthetic polymer composites in lightweight and non-structural applications.

**Keywords** *Himalayacalamus falconeri* fiber (HFs) · Mechanical properties · Vicat softening temperature (VST) · Heat deflection temperature (HDT) · Direct injection molding (DIM) · Biocomposites

## 1 Introduction

The growing environmental challenges and rising prices of petroleum-based polymers and strict environmental policies have forced scientists and researchers to rethink and develop a new class of sustainable materials [1, 2]. Green composites, made of a biodegradable matrix reinforced with bio-fibers, have the

potential to replace non-biodegradable composites for environmental sustainability and commercial viability [3–5]. Biocomposites reinforced with natural fibers are gaining popularity in various industries due to their lightweight, eco-friendly, sustainable, and biodegradable nature, as well as their favorable physicochemical, mechanical, and thermal properties. They are already being used in aerospace, automotive, sports, and home decor items [6–10]. The advances in the polymer industry have popularized the use of biopolymer composites in structural engineering applications. Biopolymer matrices like polylactic acid (PLA), poly(3-hydroxybutyrate-co-3-hydroxy valerate) (PHBV), poly(butylene succinate) (PBS), and polycaprolactone (PCL) are being investigated for their potential uses [11–13]. PLA, in particular, is gaining attraction in engineering applications, especially in automotive exterior and

✉ Mayank Pokhriyal  
mayankbpec@gmail.com

<sup>1</sup> Department of Mechanical Engineering, National Institute of Technology, Srinagar (Garhwal) 246174, Uttarakhand, India

<sup>2</sup> Department of Mechanical Engineering, Gurukula Kangri (Deemed to Be University), Haridwar 249404, Uttarakhand, India

interior parts, due to its biodegradability, attractive aesthetics, and good mechanical characteristics [14]. However, PLA has limitations in terms of cost, low heat deflection temperature, and brittleness. These limitations can be addressed by blending natural fibers and fillers with PLA matrix to improve its overall performance [15].

Natural fibers such as *Aloe vera*, bamboo, banana, mukwa, jute, sisal, Himalayan nettle, and tasar silk that are being used as a bio-reinforcement have the potential to suitably replace synthetic fiber in the polymer matrix due to their desirable properties, i.e., low density, biodegradable, non-corrosiveness, easy availability, non-toxic nature, and low carbon emission and less energy-intensive [15–29]. Using 65% hemp fibers instead of 30% glass fibers reduces energy consumption by 50,000 MJ, indicating an energy-efficient process [30]. Natural fiber utilization in plastics is projected to increase by 15–20% annually; while in the automotive and construction industries, it is expected to grow by 15–20% and 50%, respectively [31]. However, natural fibers have some disadvantages, such as reduced poor fiber-matrix interfacial interaction and low thermal performance [32]. The excessive presence of chemical constituents on the fiber surface (hemicellulose, lignin, pectin, wax) hinders interfacial bonding with the polymer matrix [33]. Several studies proposed chemical-based surface modification techniques (alkaline, silane, acetylation, peroxide, and benzylation) to overcome this barrier [34–37]. Alkali treatment is effective, affordable, and widely used to remove non-cellulosic components, improving interfacial adhesion [38–40]. However, excessive alkali concentration beyond the optimal threshold reduces biocomposite strength [41, 42]. Shiva et al. [8] found that 10% NaOH-treated fibers reduced amorphous

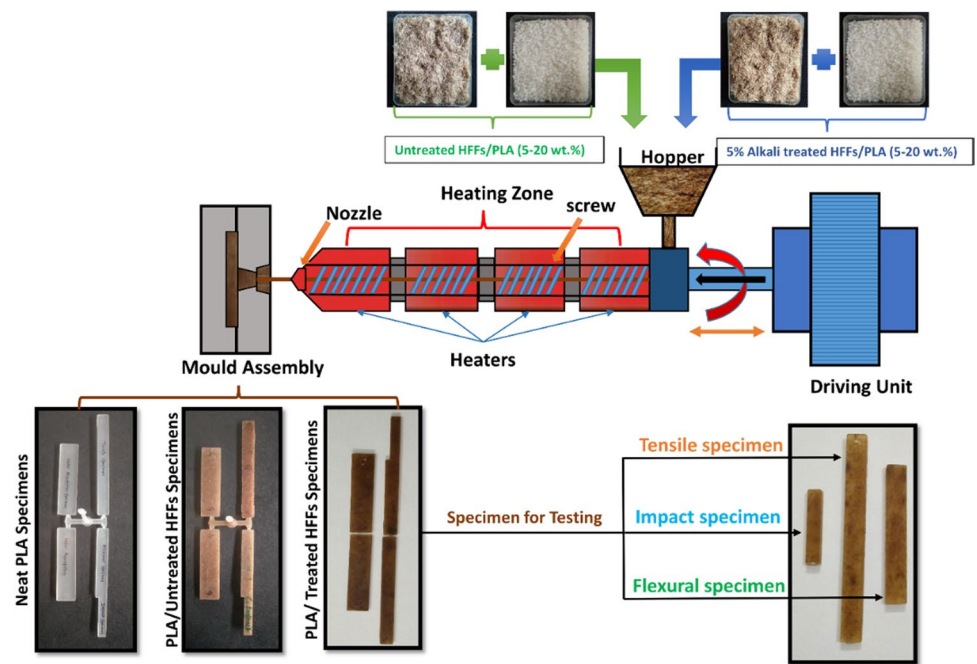
content, improving composite mechanical characteristics. Huang and Young [43] reported improved performance of bamboo/epoxy composites with alkali treatment (0.1 N NaOH, 100 °C, 12 h). Khan et al. [44] found that 6% NaOH-treated bamboo fibers showed maximum tensile strength in an epoxy matrix. Furthermore, Mwaikambo and Ansell [45] observed increased crystallinity and internal structural change in sisal fibers with alkalization.

Biocomposites may be processed in a variety of ways, including melt mixing, hand lay-up, compression molding, injection molding, spray lay-up, and resin transfer molding [46–48]. However, the commercial viability of biocomposites depends on a processing technique that is efficient, is easy to operate, and produces biocomposites with consistent dimensional qualities [49]. The selection of a suitable processing technique has a significant impact on biocomposite properties, considering variables such as production method, processing parameters, fiber dispersion and orientation, and interfacial aspects of constituent materials [50]. Injection molding is commonly used for short fiber-based composites, but extrusion is also preferred by many researchers for mixing polymer pellets and chopped natural fibers in biocomposite production. Komal et al. [49] investigated the influence of processing methods (direct injection molding (DIM), extrusion-injection molding (EIM), and extrusion compression molding (ECM)) on banana fiber/PLA biocomposites. EIM and ECM require additional operations like extrusion compounding, pelletizing, and drying at high temperatures to remove moisture, which can potentially degrade natural fibers and polymer pellets. These additional steps also increase operational time and expenses. To overcome these challenges, alternative

**Fig. 1** *Himalayacalamus falconeri* fiber undergoing **a** chopping process and **b** sieving process



**Fig. 2** Schematic of direct injection molding (DIM) process



methods like DIM (direct injection molding) may be used without compounding [50, 51]. The growing demand for biocomposites has spurred research in the design, manufacture, and characterization of their properties [52]. It has been noted that reinforced PLA composites manufactured from natural fibers exhibit properties that are on par with, or even superior to, those made from manmade fibers. Serizawa et al. [53] evaluated that the impact behavior of PLA/kenaf fiber composites ( $5.5 \text{ kJ/m}^2$ ) was equivalent to that of glass fiber/PLA composites ( $5.1 \text{ kJ/m}^2$ ) and glass fiber/ABS composites ( $4.8 \text{ kJ/m}^2$ ). Huda et al. [54] studied that PLA/RNCF/talc hybrid composites (RNCF, recycled newspaper cellulose fibers) showed significantly improved flexural strength (132 MPa) and flexural modulus (15.3 GPa) compared to unhybridized PLA/RNCF composites (77 MPa and 6.7 GPa, respectively). Xiao-Yun et al. [55] fabricated PLA/flax composites and determined that the highest strength was achieved at a flax volume percentage of 35% using the hot-pressing technique. Bajpai et al. [14] compared PLA- and PP-based composites reinforced with different natural fibers (nettle, *Grewia optiva*, sisal fiber) and reported better mechanical characteristics in PLA-based composites, suggesting its potential as a replacement for traditional fiber composites in various applications.

In the current experimental investigation, *Himalayacalamus falconeri* fiber reinforced PLA biocomposites were fabricated using direct injection molding (DIM) for the first time. The effect of NaOH treatment and

fiber concentration (5–20%) on the mechanical and thermal behavior of the biocomposites was experimentally investigated. Tensile, flexural, impact, and hardness tests were conducted according to ASTM standards for mechanical characterization. Water absorption and soil burial biodegradability tests were performed, and Vicat softening temperature (VST) and heat deflection temperature (HDT) were used to study thermal behavior. Scanning electron microscopy (SEM) was employed for fracture surface analysis. Optimum fiber concentration for *Himalayacalamus falconeri* fiber reinforced biocomposites was determined based on the findings.



**Fig. 3** Defects during direct injection molding (DIM) process, **a** flash and **b** short shot

**Table 1** Process parameters selected for direct injection molding of developed biocomposite

Parameter	Value
Temperature distribution (°C) (feed to the nozzle)	165– 175– 190– 200
Injection pressure at screw tip (MPa)	60
Injection time (s)	3
Holding pressure at the screw tip (MPa)	55
Holding time (s)	8
Mold temperature (°C)	35
Screw rotational speed (rpm)	120
Back pressure (MPa)	20

## 2 Materials and characterization

### 2.1 Materials

#### 2.1.1 Polylactic acid (PLA) as bio-matrix

Polylactic acid (PLA) (grade 3052D) in pellet form was supplied by Natur-Tec India Pvt. Ltd., Chennai, India. The biopolymer has a density of 1.24 g/cm<sup>3</sup>. The glass transition temperature ( $T_g$ ) and melting temperature ( $T_m$ ) of PLA are 55–60 °C and 200 °C, respectively. PLA pellets being hygroscopic were dried in a hot air oven at 60 °C for 2 h before mixing with natural fiber.

#### 2.1.2 *Himalayacalamus falconeri* fibers as bio-reinforcement

*Himalayacalamus falconeri* (HF), also known as Dev-Ringal or hill bamboo, is a fast-growing grass evergreen bamboo species and was procured from Rudraprayag district of Uttarakhand state, India. It can grow up to 6 m tall with a diameter of 1.5–3.5 cm and is resistant to water and cold temperatures as low as –13 °C [56, 57]. The fibers were extracted from its culms through water retting followed by a mechanical extraction process. *Himalayacalamus falconeri* fiber possesses good mechanical properties [24, 58]. The *Himalayacalamus falconeri* fiber (HFF) was chopped into the length of 3–5 mm for optimum dispersion with the resin during fabrication using direct injection molding. The chopped fibers were soaked in lukewarm water at a temperature of 40–45 °C for 3 h to separate the fiber and get rid of the pith and other impurities. The fibers were then dried in the open air for 24 h to get rid of moisture and other foul gases. The dried fiber was first filtered through a sieve (mesh no. 20 followed by mesh no. 60) to exclude the uncrushed fiber in the sieving process and then completely dried in a

hot oven (at 80 °C for 5 h). The images of HFFs undergoing the chopping and sieving process are shown in Fig. 1a, b.

### 2.2 Fiber surface modification

To investigate the effect of alkali on the properties of the biocomposites, surface modification on HF fiber was done with 5% (w/v) NaOH solution for 5 h at 30 °C. Pellets of sodium hydroxide (NaOH) were provided by Central Drug House (CDH), New Delhi, India. The fiber-to-liquid ratio was maintained at 1:20. Afterward, the treated HFFs were taken out from the alkaline solution. For a short duration of time, fibers were soaked initially in a 1% (w/v) HCl solution and then washed repeatedly until the pH was neutralized, as measured using red litmus paper. After 24 h of drying at 80 °C, this treated fiber is ready for use as bio-reinforcement with the PLA matrix.

### 2.3 Processing of biocomposites using direct injection molding machine (DIM)

The direct injection molding technique has been recognized as a commercial manufacturing option for the fabrication of biocomposite to meet market demands. PLA-based biocomposites incorporating *Himalayacalamus falconeri* fibers (HFFs) of varying fiber content (5%, 10%, 15%, and 20% by weight) were fabricated during pilot experimentation using direct injection molding process (DIM) (Model: SH-900). Manually (without compounding) mixing dried PLA pellets with short HF fibers was done before feeding them directly into the hopper of the injection molding machine. The schematic of the direct injection molding process is shown in Fig. 2. At 20 wt.% fiber content and above, a high volume of natural fiber resulted in various problems such as agglomeration of fibers, choking of the nozzle, blending difficulties, and fiber burnout, during the processing. Hence, test specimens incorporating fiber weight fractions up to 20% were manufactured as per the ASTM standard. During injection molding, process parameters such as barrel temperature and injection pressure have a considerable impact on the performance of the composites and thus must be optimized to produce high-quality parts. The fluidity of melt in the barrel and cavity can be improved by raising the temperature of the barrel; however, it may damage natural fibers and degrade polymers, and therefore this temperature needs to be optimized. On the other hand, the injection pressure must be optimized so that it does not cause flash and warpage, fiber degradation due to high shearing action in the barrel, and random orientation of fibers within the composites, all of which may result in deterioration of the performance of composites. Figure 3 shows the few defects that might occur in the specimens



**Table 2** Nomenclature of developed biocomposites

Fiber	Fiber concentration (%)	Label
PLA	0	PLA
UHF	5	PL/UHF-5
UHF	10	PL/UHF-10
UHF	15	PL/UHF-15
UHF	20	PL/UHF-20
THF	5	PL/THF-5
THF	10	PL/THF-10
THF	15	PL/THF-15
THF	20	PL/THF-20

PLA polylactic acid, UHF untreated *Himalayacalamus falconeri* fiber, THF 5% alkali-treated *Himalayacalamus falconeri* fiber

PL/UHF untreated *Himalayacalamus falconeri* fiber reinforced biocomposites

PL/THF 5% alkali-treated *Himalayacalamus falconeri* fiber reinforced biocomposites

when the manufacturing process is not optimized. Based on the results of the pilot experiments, Table 1 shows the details of the optimized parameters of the injection molding machine used to fabricate the sample. The nomenclature of biocomposites developed with varying fiber concentrations is given in Table 2.

## 2.4 Morphological characterization

Microstructure analysis of UHF, THF, and the fractured biocomposite specimens were carried out on scanning electron microscope (SEM) (Make: LEO, Model: 435P) at a resolution of 100–500 $\times$  along with a sputter coater (BAL-TEC-SCD-005). Before micrographs were taken, the specimen was coated with a thin layer of gold using a sputter coater in order to boost the specimen's conductivity.

## 2.5 Tensile properties

UTM (Make: Instron, Model: 5982) was used to measure the tensile characteristics of biocomposites according to ASTM D3039M-14 at crosshead speed of 1.5 mm/min and gauge length of 50 mm, respectively. Tensile properties were measured in terms of tensile strength and tensile modulus, at room temperature of 27 °C and relative humidity of 65%. A total of three samples (Fig. 4a) were tested for all developed biocomposites, and the average value is reported.

## 2.6 Flexural properties

All biocomposites were evaluated for flexural characteristics on UTM (Make: Instron, Model: 5982) at 2 mm/min crosshead speed and 60-mm gauge length, according to ASTM D790-10. Flexural strength and modulus were assessed. Three samples (Fig. 4b) were tested for each test and the average result is reported.

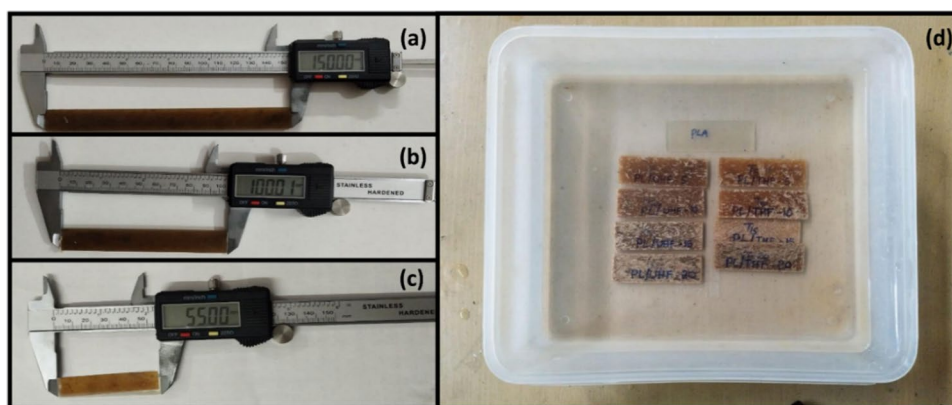
## 2.7 Impact test

Notched Izod impact test specimens were examined using a low-energy impact tester (Tinius Olsen-IT504) in accordance with ASTM D256-10. Five samples (Fig. 4c) were tested for each test, and the average value is reported.

## 2.8 Microhardness test

A Shore D hardness tester (accuracy:  $\pm 1$ ) was used to determine the hardness of pure PLA and biocomposite specimens. The resistance of a material to a spring-loaded indenter is measured in terms of its “Shore hardness.” If the number is larger, the resistance or hardness is increased. Shore D hardness is determined by taking the average of six measurements taken over the center line of the composite specimen.

**Fig. 4** Biocomposite specimens as per ASTM standard for **a** tensile test, **b** flexural test, **c** impact test, and **d** water absorption test



## 2.9 Water absorption test

As per ASTM D570-10, rectangular shape ( $76.2 \times 25.4 \times 4 \text{ mm}^3$ ) of biocomposite were cut out and put in distilled water at room temperature (Fig. 4d). The samples were heated to  $50 \text{ }^\circ\text{C}$  in a hot air oven for 24 h before being allowed to cool to room temperature in plastic bags. The specimens' dry weight ( $W_0$ ) was measured with a precision scale (Model: SES 201, Make: Saffron) that could hold up to 220 g (an accuracy of 0.0001 g). Then, the sample was submerged in distilled water for 24 h. Then, the sample was soaked in distilled water at room temperature for 24 h. Then, it was taken out of the water, wiped with tissue paper, and weighed to find its wet weight ( $W_1$ ). The rate of water absorption for the specimen was calculated using Eq. (1).

$$\text{Water absorption (\%)} = \left( \frac{W_1 - W_0}{W_0} \right) \times 100 \quad (1)$$

## 2.10 Thermal test

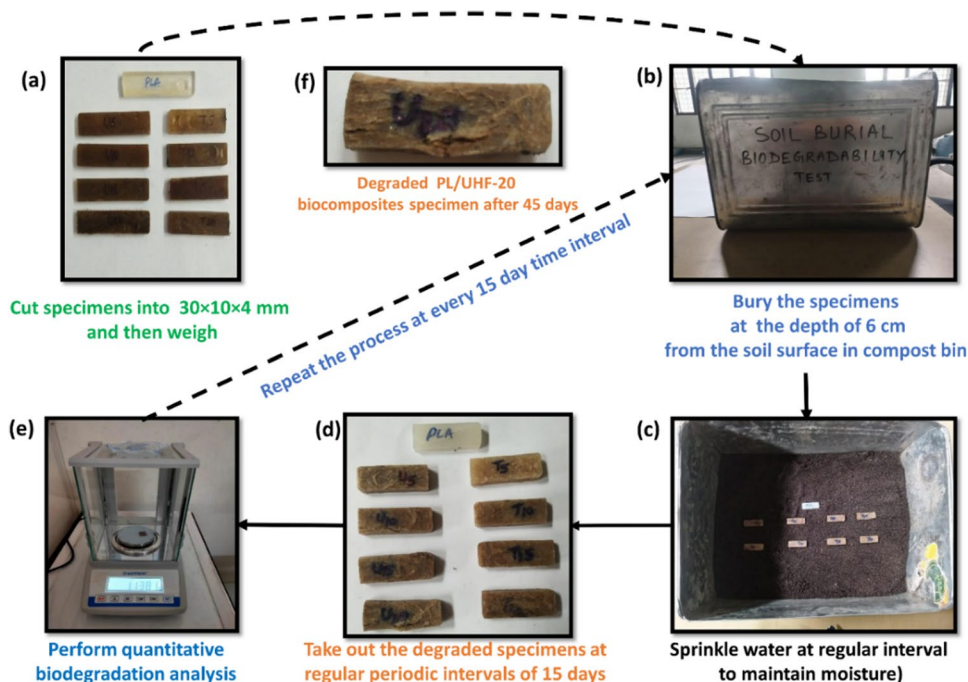
The Vicat softening temperature (VST) and heat distortion temperature (HDT) were used to measure the thermal stability of the composites. This was done with an automatic HDT/VST apparatus (Make: Coesfeld, Model: 40–190-100) with a range of up to  $300 \text{ }^\circ\text{C}$  with an accuracy of  $0.1 \text{ }^\circ\text{C}$ . For the Vicat softening point test, the sample was placed in a silicon oil bath under a 50 N load at  $30 \text{ }^\circ\text{C}$  and subsequently heated at a rate of  $50 \text{ }^\circ\text{C/h}$ , as

outlined in ASTM D1525. For each sample, the Vicat softening temperature was recorded as the temperature at which a needle could be inserted into the sample to a depth of  $1 \pm 0.1 \text{ mm}$ . For the HDT test, each sample was put on the deformation measuring device with a load of 0.45 MPa and a temperature rise of  $2 \pm 0.2 \text{ }^\circ\text{C/min}$  until the middle of the beam deflected to 0.25 mm, as described in ASTM D648. This temperature was recorded as the deflection temperature when a flexural load was applied.

## 2.11 Soil burial degradability test

A soil burial biodegradation test was performed for 45 days to evaluate the effect of alkali treatment on the biodegradability of the composite specimens (Fig. 5a). For this experiment, a compost bin (size:  $30 \times 16 \times 14 \text{ cm}^3$ ) filled with compost soil (pH 7 and RH 70–80%) was utilized (Fig. 5b). The relative humidity (RH) in the burial site was maintained by sprinkles of water at regular intervals. The composite specimens were buried at a depth of 6 cm below the surface of the soil, and the average temperature during the exposure period was  $18\text{--}20 \text{ }^\circ\text{C}$  (Fig. 5c). Every 15 days, buried samples were dug out, washed, and then dried at  $50 \text{ }^\circ\text{C}$  in a hot air oven for 5 h (Fig. 5d). The percentage of weight loss was used to assess biodegradation behavior. The weight of the specimen before and after the exposure was measured using a precision electronic balance (Model: SES 201, Make: Saffron) with an accuracy of 0.0001 g (Fig. 5e).

**Fig. 5** Soil burial degradability test procedure showing **a** cut specimens, **b** specimens buried in compost bin, **c** sprinkling of water at regular interval, **d** degraded specimens after 15 days, **e** weighing of degraded specimen, and **f** degraded PL/UHF-20 specimen after 45 days



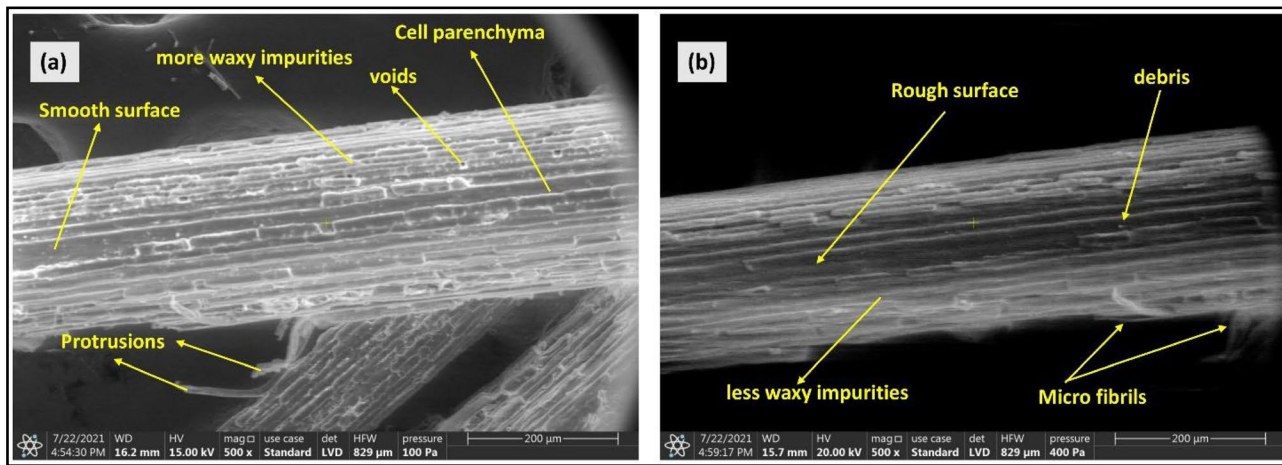


Fig. 6 SEM micrographs of **a** untreated *Himalayacalamus falconeri* fiber UHF and **b** treated *Himalayacalamus falconeri* fiber (THF)

### 3 Results and discussion

#### 3.1 Fiber morphology

The SEM micrographs for untreated *Himalayacalamus falconeri* fiber (UHF) and 5% NaOH-treated *Himalayacalamus falconeri* fiber (THF) are depicted in Fig. 6. Untreated *Himalayacalamus falconeri* fiber (UHF), as shown in Fig. 6a, contains parenchyma cells and other non-cellulosic components (wax and oil) on its surface which make it hard to form good interfacial interaction when used as reinforcing material in the polymer matrix and thereby influencing the performance of natural fiber reinforced polymer composites. To evaluate the influence of treatment on the mechanical properties of fiber

reinforced biocomposites, alkali treatment with 5% NaOH was done on the fiber surface which appeared cleaner since the weak and amorphous components that normally bind the fibers together had been removed, as shown in Fig. 6b. Consequently, the disintegration of fiber bundles into micro-fibrils occurs which improves the aspect ratio as well as the surface area accessible for bonding when reinforced with the polymer matrix, thereby affecting the performance of fiber reinforced polymer composites [59, 60].

#### 3.2 Tensile properties

Figure 7 depicts a comparison of the tensile properties of plain PLA, untreated fiber reinforced biocomposites, and treated biocomposites. The tensile properties for both

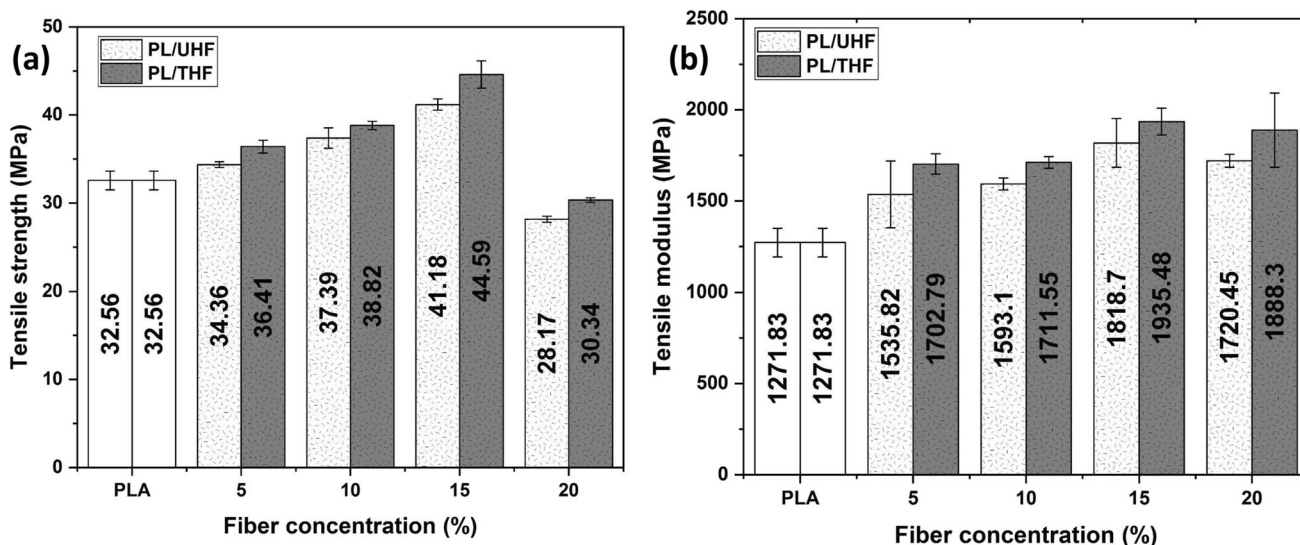


Fig. 7 Tensile properties of PLA-based UHF and THF reinforced biodegradable composites; **a** tensile strength and **b** tensile modulus



biocomposites (untreated and treated) improved with the increase in fiber concentration, reaching their highest values at 15% fiber concentration and then decreasing with a further increase in fiber concentration up to 20%. This trend may be attributed to agglomeration caused by a higher volume of fibers beyond 15 wt.%, leading to feeding and blending challenges during processing which may have further contributed to the decrease in strength of the developed composites. For both types of biocomposites (untreated and treated), biocomposite with alkali-treated fibers (PLA/THF-15) exhibited the highest tensile strength of 44.59 MPa ( $\pm 1.55$  MPa) and tensile modulus of 1935.48 MPa ( $\pm 73$  MPa), whereas the untreated biocomposite displayed a tensile strength of 41.18 MPa ( $\pm 0.64$  MPa) and tensile modulus of 1818.7 MPa ( $\pm 133$  MPa). Compared to neat PLA (32.56 MPa), the tensile strength of PL/UHF-15 biocomposites significantly improved by 26.47%, as depicted in Fig. 7a. However, incorporating alkali-treated fiber into the PLA matrix increased the tensile strength of PL/THF-15 biocomposites by 8.28% relative to PL/UHF-15 biocomposites. The tensile modulus of the developed biocomposites exhibited a substantial increase in comparison to PLA, as shown in Fig. 7b. The tensile modulus for PL/UHF-15 biocomposite surged by 43%, compared to neat PLA (1271.83 MPa). This increase in modulus implies an increased stiffness of biocomposites due to the incorporation of fiber into the PLA matrix. Furthermore, with the incorporation of alkali-treated fibers, the tensile modulus of PL/THF-15 biocomposite improved by 6.5% compared to the tensile modulus of PL/UHF-15 biocomposite. It can be concluded that alkali treatment leads to the removal of parenchyma cells and wax on the fiber surface, which results in more mechanical interlocking sites, leading to an increased interfacial bonding which further results in increased tensile strength of alkali-treated fiber reinforced biocomposites [33]. The increase in tensile

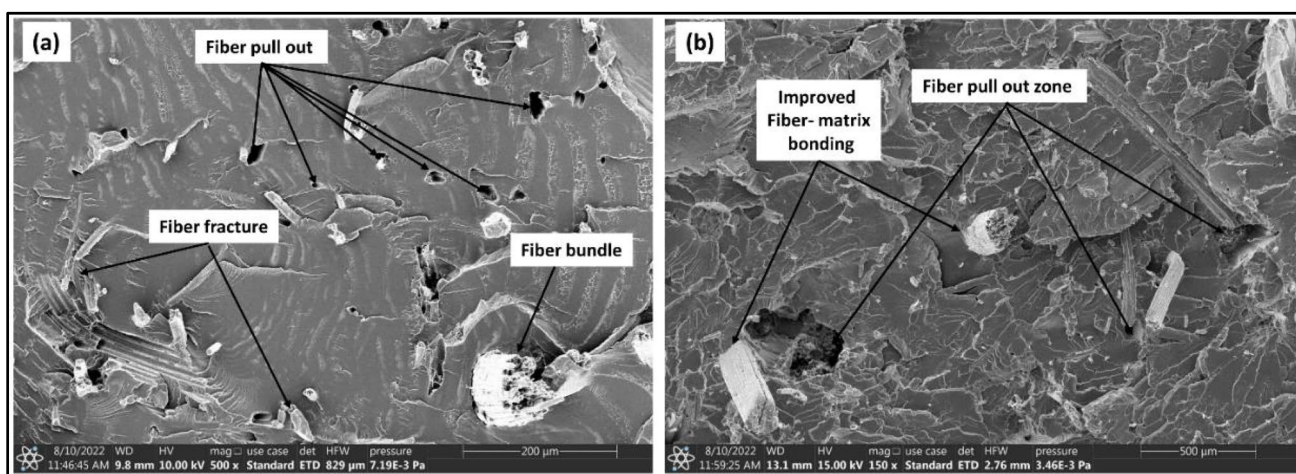
properties (strength and modulus) of PLA-based biocomposites is supported by several published research [61–63].

### 3.2.1 Morphological analysis of tensile fractographs

The fractured tensile specimens of the untreated PL/UHF-15 and treated PL/THF-15 biocomposites are shown in Fig. 8. The micrographs show that the biocomposite fails under tensile stress, with cracks appearing in the matrix, fibers breaking, and pullouts occurring in the fibers. A strong interfacial connection is essential for good tensile characteristics. The tensile qualities are governed by a small set of variables, including adhesion strength, fiber-matrix interactions, and fiber pullouts [14, 64]. In Fig. 8a, failure in PL/UHF-15 is seen as fiber pullouts, and there are zones of fiber pullouts over the fracture surface, indicating poor interfacial bonding. However, in Fig. 8b which depicts treated fiber reinforced PL/THF-15 biocomposites, the failure mode was identical but with reduced fiber pullouts and fiber breakages, showing increased fiber-matrix adhesion due to alkalization done on the fiber. It can be concluded that fiber treatment using an alkali solution enhanced fiber-to-matrix adhesion, resulting in better tensile characteristics.

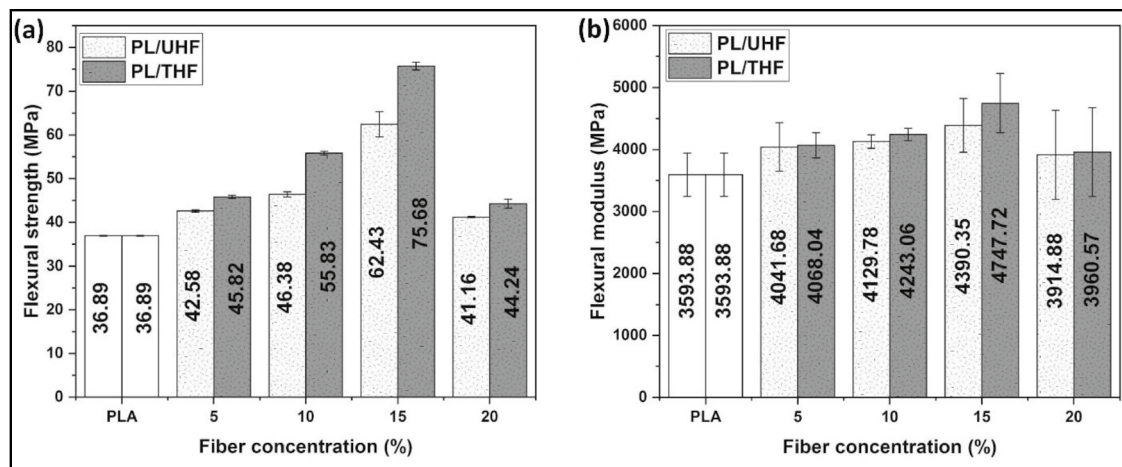
### 3.3 Flexural properties

Figure 9 shows comparative graphs of the flexural characteristics of UHF and THF fiber reinforced biocomposites in comparison to neat PLA. Flexural properties were found to be improved with fiber concentration for both untreated and treated biocomposites, reaching a maximum of 15% fiber concentration and then decreasing with further increases in fiber concentration up to 20%. For both types of biocomposites (untreated and treated), biocomposite with alkali-treated fibers (PLA/THF-15)



**Fig. 8** Tensile test fractographs of **a** PL/UHF-15 and **b** PL/THF-15





**Fig. 9** Flexural properties of PLA-based UHF and THF reinforced biodegradable composites; **a** flexural strength and **b** flexural modulus

demonstrated superior flexural performance, with a maximum flexural strength of 75.68 MPa ( $\pm 0.88$  MPa) and flexural modulus of 4747.72 MPa ( $\pm 477.08$  MPa) at 15 wt.% fiber content, compared to the untreated biocomposite which showed a flexural strength of 62.43 MPa ( $\pm 2.89$  MPa) and flexural modulus of 4390.35 MPa ( $\pm 433.58$  MPa). The maximum flexural strength is shown by PL/UHF-15 and PL/THF-15 with an improvement of 69.80% and 105.15%, respectively, compared to neat PLA (36.89 MPa) as depicted in Fig. 9a. It is worth noting that compared to untreated fiber, flexural strength was even further increased when alkali-treated fiber was used. When PL/THF-15 is compared with PL/UHF-15, there was an improvement of 21.22% in the flexural strength of developed composites. Furthermore, the addition of alkali-treated fiber enhanced the flexural modulus of the treated fiber reinforced biocomposites as depicted in Fig. 9b. The flexural modulus of treated fiber reinforced PL/THF-15 biocomposites increased by 8.13% compared to untreated fiber reinforced PL/UHF-15 biocomposites. When compared to neat PLA, the flexural modulus of PL/UHF-15 and PL/THF-15 biocomposites improved by 22.16% and 32.10%, respectively. This increased stiffness can be attributed to better stress transfer between the stiff fiber and PLA matrix along with better distribution of reinforcement within the PLA matrix. Moreover, post-alkali treatment disintegrates the fiber bundles into fiber fibrils resulting in an increased aspect ratio and surface area available for bonding with the PLA matrix to ensure better wettability [65, 66]. It is worth noting that the injection pressure used during manufacturing helps in the improvement of fiber orientation in the flow direction, which improves the modulus of the developed composites [67, 68].

### 3.3.1 Morphological analysis of flexural fractographs

The flexural test fractographs of PL/UHF-15 and PL/THF-15 are shown in Fig. 10. The flexural properties of biocomposites are mostly determined by the bonding at the interphase. Flexural strength is also dependent on the proper ratio of reinforcement, fiber treatment, and fabrication methods [69–71]. PL/UHF-15 and PL/THF-15 showed maximum flexural strength and modulus at 15% fiber concentration. Figure 10a illustrates micrographs of fiber fracture, debonding, and matrix fractures in untreated fiber reinforced PL/UHF-15 biocomposites. Better flexural characteristics are shown in alkali-treated fiber-reinforced PL/THF-15 biocomposites due to enhanced fiber-matrix bonding as shown in Fig. 10b.

### 3.4 Impact properties

The impact strength of the biocomposites majorly depends on factors such as type of fiber, treatment on fiber, fiber distribution within the matrix, fiber-matrix adhesion, and toughness of fiber and matrix. The impact strength of a material is associated with the energy consumed during fracture, which may result from fiber fracture, fiber-matrix debonding, and fiber pullouts [15, 72, 73]. From Fig. 11a, it is evident that the notched impact strength of all the biocomposites increases with an initial increase in fiber concentration, becomes maximum at 15% fiber concentration, and then decreases with further increase in fiber concentration up to 20%. Compared to neat PLA, the notched impact strength of all the fabricated biodegradable composites significantly improved with the incorporation of UHF and THF. During impact testing, PLA-based biocomposite specimens were fractured into two pieces, confirming the brittleness of

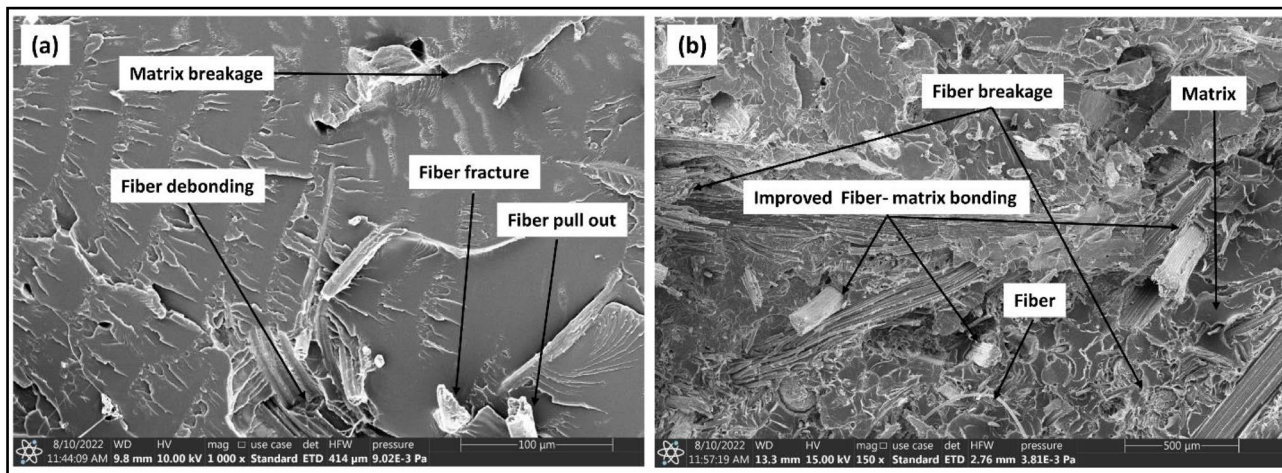


Fig. 10 Flexural test fractographs of **a** PL/UHF-15 and **b** PL/THF-15

the PLA matrix. Within untreated and treated biocomposites, PL/UHF-15 and PL/THF-15 showed the highest value of notched impact strength compared to PLA (30.82 J/m) with an improvement of 35.88% and 35.04%, respectively. In addition, all the treated biocomposites (PL/THF) exhibited a reduced impact strength compared to the untreated biocomposites (PL/UHF). The impact strength of PL/THF-15 (41.62 J/m) declined by 0.62% compared to the impact strength of PL/UHF-15(41.88 J/m). The good fiber-matrix adhesion in treated biocomposites (PL/THF) causes more fiber breakages than fiber pullouts during impact loading, reducing impact strength [15]. It is noteworthy that energy lost due to fiber breakage is lower than energy lost due to fiber pullouts. Additionally, treated biocomposites have

more fiber fibril ends than untreated biocomposites, which operate as stress concentration points and increase crack propagation, thereby reducing impact strength [74]. Even though the impact strength of PL/UHF-20 and PL/THF-20 biocomposites decreased at 20% fiber concentration, their impact strength was still higher than PLA by 25.21% and 10.90%, respectively. Thus, it may be concluded that the untreated composite had weaker interfacial bonding, which aided in releasing more energy owing to fiber pullouts.

### 3.4.1 Morphological analysis of impact fractographs

Figure 12 shows impact test fractographs of PL/UHF-15 and PL/THF-15 biocomposites. Figure 12a shows that there

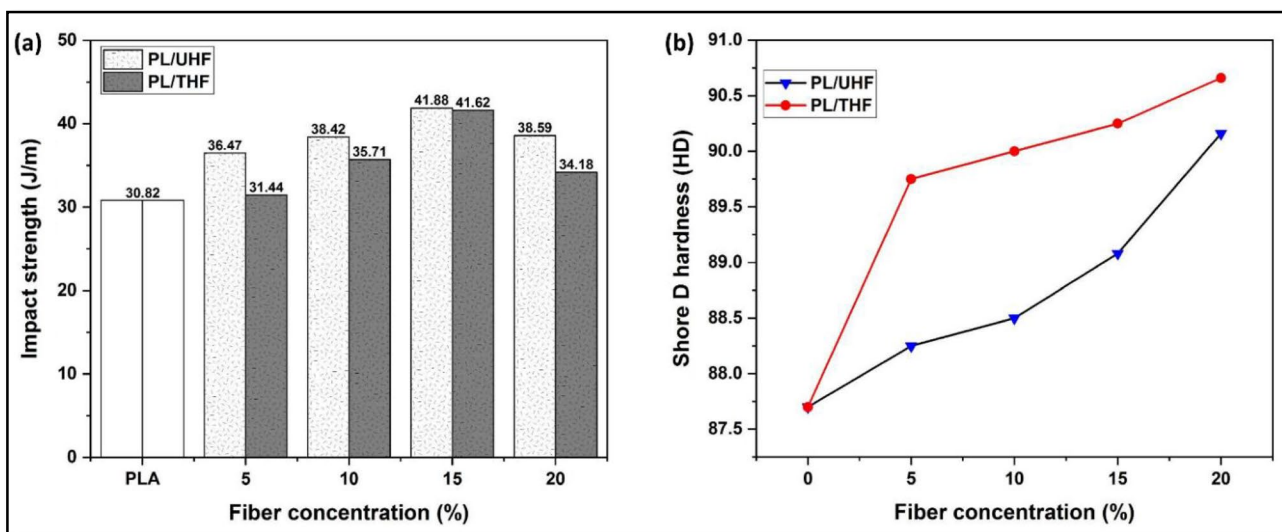
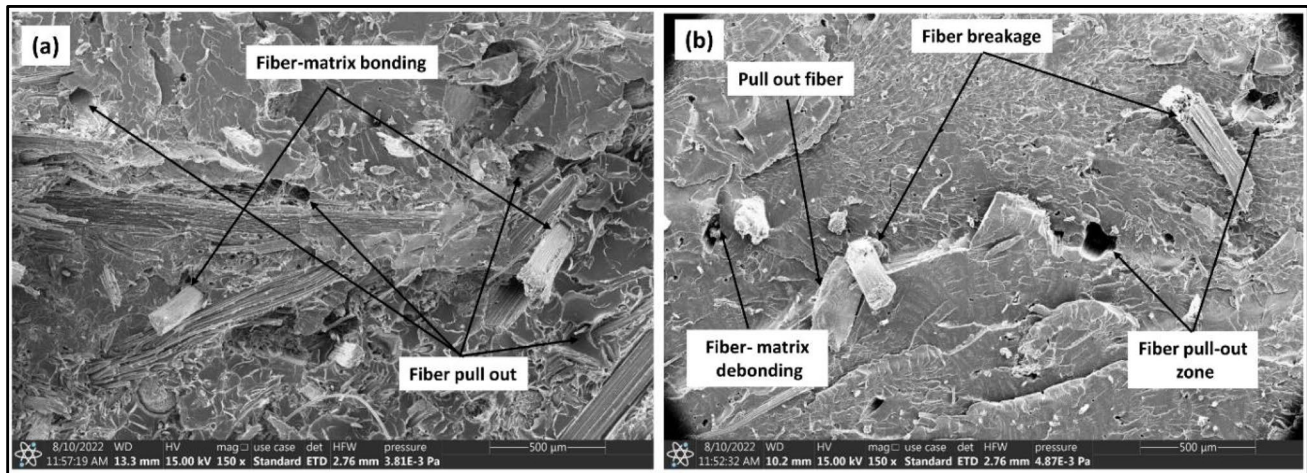


Fig. 11 PLA-based UHF and THF reinforced biocomposites. **a** Impact properties and **b** Shore D hardness values



**Fig. 12** Impact test fractographs of **a** PL/UHF-15 and **b** PL/THF-15

are more fiber pullout regions in untreated biocomposites (PL/UHF-15) due to low or medium interfacial adhesion between fiber and matrix. The untreated fiber generally has wax and non-cellulosic content on its surface which lead to poor fiber-matrix adhesion which is responsible for a greater number of fiber pullouts rather than fiber breakage. After alkalization, the fiber surface gets improved resulting in good interfacial interaction with the PLA matrix. So, in the case of treated biocomposites (PL/THF-15), more fiber breaks are seen than fiber pullouts, as shown in Fig. 12b. This means that treated biocomposites have a lower impact strength. Therefore, in the case of treated biocomposites (PL/THF-15), more fiber breakage is seen than fiber pullouts, as illustrated in Fig. 12b, leading to a decrease in impact strength.

### 3.5 Microhardness test

Figure 11b shows that the addition of both raw and treated fiber considerably improved the hardness value of all the fabricated biocomposites. In both types, untreated and treated fiber reinforced biocomposites, biocomposite treated with alkali (PLA/THF-15) at a fiber content of 20 wt.% displayed the highest hardness value of 90.66 HD ( $\pm 0.60$ ), whereas the untreated biocomposite (PL/UHF-20) showed a hardness of 90.16 HD ( $\pm 0.68$ ). The maximum hardness values were observed for PL/UHF-20 and PL/THF-20 which were marginally improved by 2.8% and 3.3%, respectively, compared to neat PLA (87.7 HD). The possible reason for this increased hardness may be the incorporation of stiffer fibers into the PLA matrix, which is brittle. In addition, alkali-treated fiber reinforced PL/UHF-20 biocomposite showed improved hardness by 5.45%, compared to untreated fiber reinforced PL/UHF-20 biocomposites. This increased hardness values for PL/THF compared to PL/UHF can be

attributed to improved chemical bonding at fiber-matrix interphase due to fiber fibrillation and removal of non-cellulosic content from the fiber surface which led to less micro-voids and fiber debonding in the interphase region thereby improve the compatibility, which in turn, ensures the higher hardness values.

### 3.6 Water absorption properties

Water absorption behavior of pure PLA, untreated fiber biocomposites, and 5% alkali-treated biocomposites were evaluated by measuring the percentage of weight gain over time when submerged in distilled water at room temperature, as presented in Fig. 13. The water absorption capacity of biocomposites depends on the factors such as fiber properties, fiber treatment, and fiber-matrix interfacial properties. It is observed that the water absorption rate of the biocomposites increases with increasing the fiber concentration as depicted in Fig. 13a, b. Among all the developed biocomposites, the lowest water absorption rate is shown by neat PLA biocomposite which is 0.32%. The maximum weight gain for untreated and treated biocomposites is 2.60% and 2.42% for PL/UHF-20 and PL/THF-20, respectively. The weight gain is highest at 20% fiber concentration, resulting in the interlocking of a large number of water molecules in the biocomposites. The water molecules then assault the interface, debonding the fiber and PLA matrix at the interface as depicted in Fig. 13c. It is observed that untreated biocomposites (PL/UHF) absorbed more water than 5% alkali-treated biocomposites (PL/THF) due to the hydrophilic nature of untreated *Himalayacalamus falconeri* fiber and the presence of an amorphous material such as wax and oil on the fiber surface which is responsible for low or medium interfacial interaction between fiber and PLA matrix [75–77]. It can be evident that the initial water absorption rate for both



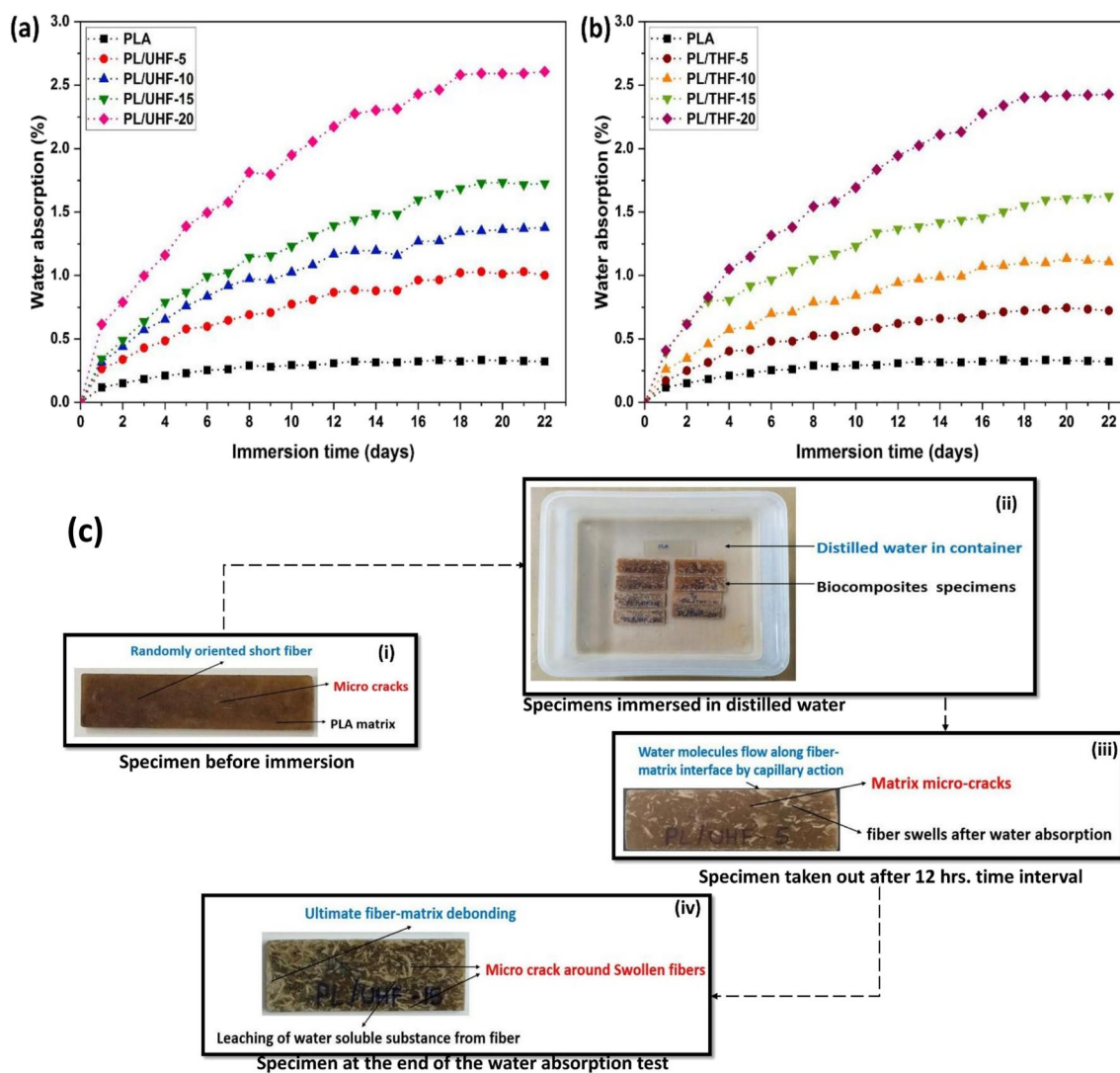


**Fig. 13** Water absorption rate of **a** untreated biocomposites, **b** 5% alkali-treated biocomposites, and **c** water absorption mechanism showing **i** specimen before immersion, **ii** specimen immersed in dis-

tilled water, **iii** specimen taken out after 12 hrs. time interval and **iv** specimen at the end of water absorption test

untreated and treated biocomposites increased quickly in the first few days and then slowed down after 10 days. After approximately 19 days, the water absorption percentage of all developed biocomposites becomes saturated.

### 3.7 Thermal analysis

The Vicat softening temperature (VST) and heat deflection temperature (HDT) of all the developed biocomposites are depicted in Fig. 14. It is observed that the VST of developed biocomposites increased with increasing the fiber concentration as shown in Fig. 14a. In the case of UHF and THF reinforced biocomposites, the VST for PL/UHF-20 and PL/THF-20 was found to be maximum with an increase of 3.90% and 6.27%, respectively, compared to the VST of neat PLA (53.35 °C). However, in the case of treated fiber reinforced

biocomposites, an increase in the VST value was noticed for all the fiber concentrations. This increase in VST can be explained by the possibility that the reinforcing material or fiber treatment has a restricting influence on chain mobility inside the PLA matrix. This occurs because of the insertion of fibers into the PLA matrix, which disperses and interlaces inside the matrix to produce a network structure with various linkages [78–80]. Figure 14b shows the HDT of the PLA, UHF, and THF reinforced biocomposites. The temperature of deflection under load (HDT) of UHF and THF reinforced biocomposites increased by 0.17% and 3.13%, respectively, as compared to PLA (55.8 °C). The incorporation of fiber into a PLA matrix has a marginal effect on its HDT values, although fiber treatment has considerably raised the HDT value of treated biocomposite (PL/THF-15). It can be concluded that the thermal dimensional stability of (PL/THF)

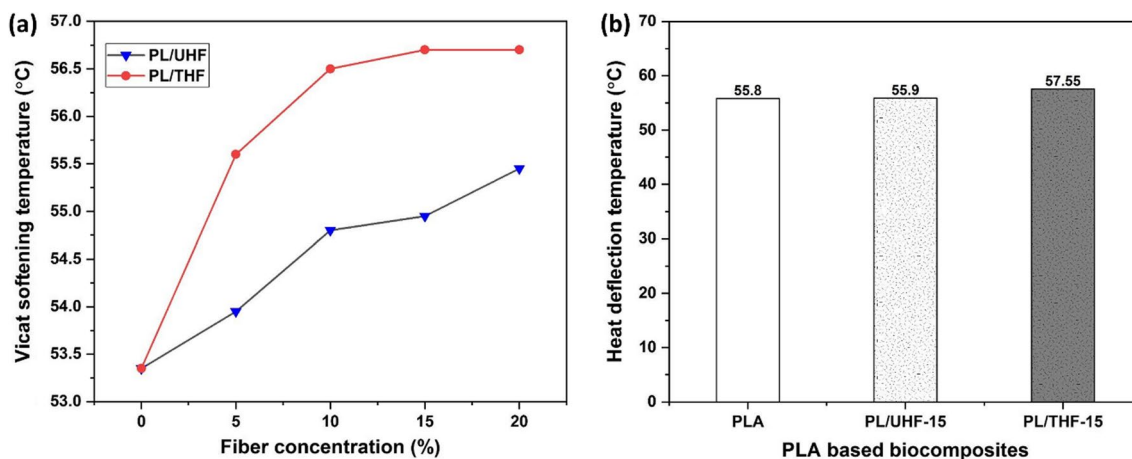


**Fig. 14** Effect of alkali treatment on **a** Vicat softening temperature and **b** heat deflection temperature of PLA-based UHF and THF reinforced biocomposites

treated biocomposites showed greater value compared to that of (PL/UHF) untreated biocomposites, enabling the application of these (PL/THF) alkali-treated biocomposites at considerably higher temperatures.

### 3.8 Biodegradability test

The percentage of weight loss was used to determine the degradation behavior of all biocomposite specimens buried in compost soil. From Fig. 15, it can be observed that the incorporation of fiber into the polylactic acid (PLA) matrix has significantly enhanced the degradation rate of the biocomposites, with the most pronounced effect observed at a fiber content of 20 wt.%, thereby promoting their eco-friendly characteristics. However, through the strategic employment of an alkalization process, the degradation rate of these biocomposites can be effectively mitigated,

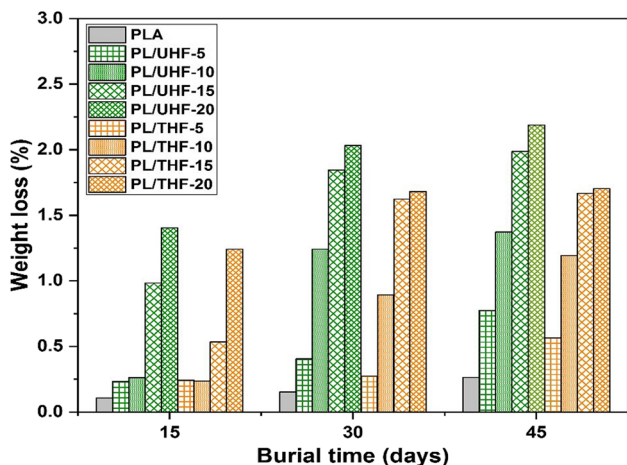


**Fig. 15** Soil burial biodegradability behavior of all developed biocomposites

showcasing a promising approach for controlling their biodegradability. Remarkably, in the case of untreated fiber (UHF) and alkali-treated fiber (THF) reinforced biocomposites, the maximum specific weight loss was observed in PL/UHF-20 and PL/THF-20, with a significant increase of 2.18% and 1.70%, respectively. In stark contrast, the neat PLA exhibited a considerably lower specific weight loss of 0.26%. The possible reason may be the high fiber concentration on the surface of biocomposite may soak up water from the moist compost soil, causing the fibers to swell and thus resulting in weak fiber-matrix interaction. Moreover, the bacteria in the moist soil are attacking the surface of the composite and causing damage to the biocomposites [81–83]. Due to the alkalization of the fiber, PL/THF reinforced biocomposites have a lower weight loss % than PL/UHF reinforced biocomposites. These findings highlight the tremendous potential of utilizing fiber-reinforced PLA composites for environmentally conscious applications.

## 4 Conclusions

In the current experimental endeavor, novel *Himalayacalamus falconeri* fiber reinforced polylactic acid (PLA) biocomposites were developed via direct injection molding, varying fiber concentration (5–20%), and alkali treatment (5% w/v NaOH solution). *Himalayacalamus falconeri* fibers (UHF and THF) significantly improved the mechanical and thermal properties of the biocomposites. Alkali treatment (5% w/v NaOH) effectively removed contaminants from the fiber surface, enhancing tensile, flexural characteristics, and impact strength. Maximum tensile, flexural, and impact properties were observed at 15 wt.% fiber concentration. Shore D hardness peaked at 20 wt.% fiber concentration. Fractured surfaces revealed various failure modes including fiber fracture, fiber pullout, matrix cracking, matrix breaking,

fiber breakage, and debonding that were depicted through SEM images. HDT values were marginally affected by fiber incorporation but significantly raised by fiber treatment in PL/THF-15 biocomposite. Soil burial degradation rate was highest for PL/UHF-20. Short *Himalayacalamus falconeri* fiber has the potential to be used as reinforcement in PLA matrix to fabricate fully biodegradable green composites, replacing synthetic polymer composites in lightweight and non-structural applications. Processing technology with short processing time, simplicity, and reproducibility should be selected for environmental sustainability and economic feasibility.

**Acknowledgements** The authors would like to thank Prof. Pankaj Madan, Gurukula Kangri (Deemed to be University), Haridwar, Uttarakhand, for providing the necessary facilities to carry out this research work. The authors would also like to thank Prof. Inderdeep Singh, Department of Industrial and Mechanical Engineering, IIT Roorkee, to carry out test facilities.

**Author contribution** Mayank Pokhriyal: Conceptualization, methodology, writing — original draft preparation. Pawan Kumar Rakesh: Investigation, reviewing and editing, and visualization.

**Funding** This work is financially supported by the Design Innovation Center (letter number 15–9/2017-PN-1), Ministry of Education, Government of India.

**Data availability** Not applicable.

## Declarations

**Ethical approval** Not applicable.

**Competing interests** The authors declare no competing interests.

## References

- Chin SC, Tee KF, Tong FS et al (2020) Thermal and mechanical properties of bamboo fiber reinforced composites. *Mater Today Commun* 23:100876. <https://doi.org/10.1016/j.mtcomm.2019.100876>
- Agarwal J, Sahoo S, Mohanty S, Nayak SK (2020) Progress of novel techniques for lightweight automobile applications through innovative eco-friendly composite materials: a review. *J Thermoplast Compos Mater* 33:978–1013. <https://doi.org/10.1177/0892705718815530>
- Khalil HPSA, Bhat IUH, Jawaid M et al (2012) Bamboo fibre reinforced biocomposites: a review. *Mater Des* 42:353–368. <https://doi.org/10.1016/j.matdes.2012.06.015>
- Bajpai PK, Singh I, Madaan J (2014) Development and characterization of PLA-based green composites: a review. *J Thermoplast Compos Mater* 27:52–81. <https://doi.org/10.1177/0892705712439571>
- Mohanty AK, Misra M, Drzal LT (2002) Sustainable bio-composites from renewable resources: opportunities and challenges in the green materials world. *J Polym Environ* 10:19–26. <https://doi.org/10.1023/A:1021013921916>
- Sanjay MR, Siengchin S, Parameswaranpillai J et al (2019) A comprehensive review of techniques for natural fibers as reinforcement in composites: preparation, processing and characterization. *Carbohydr Polym* 207:108–121. <https://doi.org/10.1016/j.carbpol.2018.11.083>
- Santhosh N, Praveena BA, Srikanth HV, et al (2022) Experimental investigations on static, dynamic, and morphological characteristics of bamboo fiber-reinforced polyester composites. *Int J Polym Sci* 2022. <https://doi.org/10.1155/2022/1916877>
- Siva R, Valarmathi TN, Samrot AV, Jeya Jeevahan J (2021) Surface-modified and untreated *Cissus quadrangularis* reinforced polylactic composite. *Curr Res Green Sustain Chem* 4:100121. <https://doi.org/10.1016/j.crgsc.2021.100121>
- Joshi SV, Drzal LT, Mohanty AK, Arora S (2004) Are natural fiber composites environmentally superior to glass fiber reinforced composites? *Compos Part A Appl Sci Manuf* 35:371–376. <https://doi.org/10.1016/j.compositesa.2003.09.016>
- Cavalcanti DKK, Banea MD, Neto JSS et al (2019) Mechanical characterization of intralaminar natural fibre-reinforced hybrid composites. *Compos Part B Eng* 175:107149. <https://doi.org/10.1016/j.compositesb.2019.107149>
- Lau K, tak, Hung P yan, Zhu MH, Hui D, (2018) Properties of natural fibre composites for structural engineering applications. *Compos Part B Eng* 136:222–233. <https://doi.org/10.1016/j.compositesb.2017.10.038>
- Akos NI, Wahit MU, Mohamed R, Yussuf AA (2013) Comparative studies of mechanical properties of poly( $\epsilon$ -caprolactone) and poly(lactic acid) blends reinforced with natural fibers. *Compos Interfaces* 20:459–467. <https://doi.org/10.1080/15685543.2013.807158>
- Ali Akbari Ghavimi S, Ebrahimzadeh MH, Solati-Hashjin M, Abu Osman NA (2015) Polycaprolactone/starch composite: fabrication, structure, properties, and applications. *J Biomed Mater Res - Part A* 103:2482–2498. <https://doi.org/10.1002/jbm.a.35371>
- Bajpai PK, Singh I, Madaan J (2012) Comparative studies of mechanical and morphological properties of polylactic acid and polypropylene based natural fiber composites. *J Reinf Plast Compos* 31:1712–1724. <https://doi.org/10.1177/0731684412447992>
- Chaitanya S, Singh I (2016) Novel Aloe vera fiber reinforced biodegradable composites - development and characterization. *J Reinf Plast Compos* 35:1411–1423. <https://doi.org/10.1177/0731684416652739>
- Zhang K, Wang F, Liang W, et al (2018) Thermal and mechanical properties of bamboo fiber reinforced epoxy composites. *Polymers (Basel)* 8. <https://doi.org/10.3390/polym10060608>
- Liu L, Yu J, Cheng L, Yang X (2009) Biodegradability of poly(butylene succinate) (PBS) composite reinforced with jute fibre. *Polym Degrad Stab* 94:90–94. <https://doi.org/10.1016/j.polymdegradstab.2008.10.013>
- Torres FG, Arroyo OH, Gomez C (2007) Processing and mechanical properties of natural fiber reinforced thermoplastic starch biocomposites. *J Thermoplast Compos Mater* 20:207–223. <https://doi.org/10.1177/0892705707073945>
- Pokhriyal M, Prasad L, Raturi HP (2017) An experimental investigation on mechanical and tribological properties of Himalayan nettle fiber composite. *J Nat Fibers* 00:1–10. <https://doi.org/10.1080/15440478.2017.1364202>
- Pokhriyal M, Prasad L, Rakesh PK, Raturi HP (2018) Influence of fiber loading on physical and mechanical properties of Himalayan nettle fabric reinforced polyester composite. *Mater Today Proc* 5:16973–16982. <https://doi.org/10.1016/j.matpr.2018.04.101>
- Ranakoti L, Rakesh PK (2020) Physio-mechanical characterization of tasar silk waste/jute fiber hybrid composite. *Compos Commun* 22:100526. <https://doi.org/10.1016/j.coco.2020.100526>



22. Hassan MZ, Roslan SA, Sapuan SM et al (2020) Mercerization optimization of bamboo (*Bambusa vulgaris*) fiber-reinforced epoxy composite structures using a Box-Behnken design. *Polymers (Basel)* 12:1–19. <https://doi.org/10.3390/POLYM12061367>
23. Lods L, Richmond T, Dandurand J et al (2022) Continuous bamboo fibers/fire-retardant polyamide 11: dynamic mechanical behavior of the biobased composite. *Polymers (Basel)* 14:1–14. <https://doi.org/10.3390/polym14020299>
24. Pokhriyal M, Kumar P (2022) Materials toda : proceedings mechanical and microstructural behaviour of NaOH treated Himalayacalamus falconeri fibers as biodegradable reinforcing material in polymer based composites. *Mater Today Proc* 62(2):1078–1082. <https://doi.org/10.1016/j.matpr.2022.04.295>
25. Rocky BP, Thompson AJ (2018) Production of natural bamboo fibers-I: experimental approaches to different processes and analyses. *J Text Inst* 109:1381–1391. <https://doi.org/10.1080/00405000.2018.1482639>
26. Komal UK, Verma V, Ashwani T et al (2020) Effect of chemical treatment on thermal, mechanical and degradation behavior of banana fiber reinforced polymer composites. *J Nat Fibers* 17:1026–1038. <https://doi.org/10.1080/15440478.2018.1550461>
27. Komal UK, Lila MK, Singh I (2020) PLA/banana fiber based sustainable biocomposites: a manufacturing perspective. *Compos Part B Eng* 180:107535. <https://doi.org/10.1016/j.compositesb.2019.107535>
28. Setswalo K, Oladijo OP, Namoshe M et al (2022) The mechanical properties of alkali and laccase treated *Pterocarpus angolensis* (mukwa)-polylactic acid (PLA) composites. *Int J Biol Macromol* 217:398–406. <https://doi.org/10.1016/j.ijbiomac.2022.07.075>
29. Yang Y, Murakami M, Hamada H (2012) Molding method, thermal and mechanical properties of jute/PLA injection molding. *J Polym Environ* 20:1124–1133. <https://doi.org/10.1007/s10924-012-0565-8>
30. Venkateshwaran N, Elayaperumal A (2010) Banana fiber reinforced polymer composites - a review. *J Reinf Plast Compos* 29:2387–2396. <https://doi.org/10.1177/0731684409360578>
31. Malkapuram R, Kumar V, Singh Negi Y (2009) Recent development in natural fiber reinforced polypropylene composites. *J Reinf Plast Compos* 28:1169–1189. <https://doi.org/10.1177/0731684407087759>
32. Gassan J, Gutowski VS (2000) Effects of corona discharge and UV treatment on the properties of jute-fibre epoxy composites. *Compos Sci Technol* 60:2857–2863. [https://doi.org/10.1016/S0266-3538\(00\)00168-8](https://doi.org/10.1016/S0266-3538(00)00168-8)
33. Kabir MM, Wang H, Lau KT, Cardona F (2012) Chemical treatments on plant-based natural fibre reinforced polymer composites: an overview. *Compos Part B Eng* 43:2883–2892. <https://doi.org/10.1016/j.compositesb.2012.04.053>
34. Mukhopadhyay S, Figueiro R (2009) Physical modification of natural fibers and thermoplastic films for composites - a review. *J Thermoplast Compos Mater* 22:135–162. <https://doi.org/10.1177/0892705708091860>
35. Mohanty AK, Khan MA, Hinrichsen G (2000) Surface modification of jute and its influence on performance of biodegradable jute-fabric/Biopol composites. *Compos Sci Technol* 60:1115–1124. [https://doi.org/10.1016/S0266-3538\(00\)00012-9](https://doi.org/10.1016/S0266-3538(00)00012-9)
36. Kalia S, Kaith BS, Kaur I (2009) Pretreatments of natural fibers and their application as reinforcing material in polymer composites—a review. *Polym Eng Sci* 1–10. <https://doi.org/10.1002/pen>
37. Gomes A, Matsuo T, Goda K, Ohgi J (2007) Development and effect of alkali treatment on tensile properties of curaua fiber green composites. *Compos Part A Appl Sci Manuf* 38:1811–1820. <https://doi.org/10.1016/j.compositesa.2007.04.010>
38. Li X, Tabil LG, Panigrahi S (2007) Chemical treatments of natural fiber for use in natural fiber-reinforced composites: a review. *J Polym Environ* 15:25–33. <https://doi.org/10.1007/s10924-006-0042-3>
39. De Rosa IM, Kenny JM, Maniruzzaman M et al (2011) Effect of chemical treatments on the mechanical and thermal behaviour of okra (*Abelmoschus esculentus*) fibres. *Compos Sci Technol* 71:246–254. <https://doi.org/10.1016/j.compscitech.2010.11.023>
40. Chen H, Yu Y, Zhong T et al (2017) Effect of alkali treatment on microstructure and mechanical properties of individual bamboo fibers. *Cellulose* 24:333–347. <https://doi.org/10.1007/s10570-016-1116-6>
41. Vinod A, Vijay R, Lenin Singaravelu D et al (2022) Effect of alkali treatment on performance characterization of *Ziziphus mauritiana* fiber and its epoxy composites. *J Ind Text* 51:2444S–2466S. <https://doi.org/10.1177/1528083720942614>
42. Sentharamaikannan P, Saravanakumar SS (2023) Evaluation of characteristic features of untreated and alkali-treated cellulosic plant fibers from *Mucuna atropurpurea* for polymer composite reinforcement. *Biomass Convers Biorefinery*. <https://doi.org/10.1007/s13399-022-03736-y>
43. Huang JK, Bin YW (2019) The mechanical, hygral, and interfacial strength of continuous bamboo fiber reinforced epoxy composites. *Compos Part B Eng* 166:272–283. <https://doi.org/10.1016/j.compositesb.2018.12.013>
44. Khan Z, Yousif BF, Islam M (2017) Fracture behaviour of bamboo fiber reinforced epoxy composites. *Compos Part B Eng* 116:186–199. <https://doi.org/10.1016/j.compositesb.2017.02.015>
45. Mwaikambo LY, Ansell MP (2002) Chemical modification of hemp, sisal, jute, and kapok fibers by alkalization. *J Appl Polym Sci* 2222–2234. <https://doi.org/10.1002/app.10460>
46. Annicchiarico D, Alcock JR (2014) Review of factors that affect shrinkage of molded part in injection molding. *Mater Manuf Process* 29:662–682. <https://doi.org/10.1080/10426914.2014.880467>
47. Cheung HY, Lau KT, Pow YF et al (2010) Biodegradation of a silkworm silk/PLA composite. *Compos Part B Eng* 41:223–228. <https://doi.org/10.1016/j.compositesb.2009.09.004>
48. Jonoobi M, Harun J, Mathew AP, Oksman K (2010) Mechanical properties of cellulose nanofiber (CNF) reinforced polylactic acid (PLA) prepared by twin screw extrusion. *Compos Sci Technol* 70:1742–1747. <https://doi.org/10.1016/j.compscitech.2010.07.005>
49. Komal UK, Lila MK, Singh I (2021) Processing of PLA/pineapple fiber based next generation composites. *Mater Manuf Process* 36:1677–1692. <https://doi.org/10.1080/10426914.2021.1942904>
50. Azad R, Shahrajabian H (2019) Experimental study of warp and shrinkage in injection molding of HDPE/rPET/wood composites with multiobjective optimization. *Mater Manuf Process* 34:274–282. <https://doi.org/10.1080/10426914.2018.1512123>
51. Rabbi MS, Islam T, Islam GMS (2021) Injection-molded natural fiber-reinforced polymer composites—a review. *Int J Mech Mater Eng* 16:1–21. <https://doi.org/10.1186/s40712-021-00139-1>
52. Bledzki AK, Jaszkiwicz A, Scherzer D (2009) Mechanical properties of PLA composites with man-made cellulose and abaca fibres. *Compos Part A Appl Sci Manuf* 40:404–412. <https://doi.org/10.1016/j.compositesa.2009.01.002>
53. Serizawa S, Inoue K, Iji M (2006) Kenaf-fiber-reinforced poly(lactic acid) used for electronic products. *J Appl Polym Sci* 100:618–624. <https://doi.org/10.1002/app.23377>
54. Huda MS, Drzal LT, Mohanty AK, Misra M (2007) The effect of silane treated- and untreated-talc on the mechanical and physico-mechanical properties of poly(lactic acid)/newspaper fibers/talc hybrid composites. *Compos Part B Eng* 38:367–379. <https://doi.org/10.1016/j.compositesb.2006.06.010>
55. Xiao-Yun W, Qiu-Hong W, Gu H (2010) Research on mechanical behavior of the flax/polyactic acid composites. *J Reinf Plast Compos* 29:2561–2567. <https://doi.org/10.1177/0731684409355201>

56. Kumar B (2009) Ringal (a dwarf bamboo): resource use pattern. *Rep Opin* 1:1–5
57. Bag N, Chandra S, Palni LMS, Nandi SK (2000) Micropropagation of Dev-ringal [*Thamnocalamus spathiflorus* (Trin.) Munro] — a temperate bamboo, and comparison between in vitro propagated plants and seedlings. *Plant Sci* 156:125–135
58. Pokhriyal M, Kumar P, Sanjay R et al (2023) Effect of alkali treatment on novel natural fiber extracted from *Himalayacalamus falconeri* culms for polymer composite applications. *Biomass Convers Biorefinery*. <https://doi.org/10.1007/s13399-023-03843-4>
59. Li Z, Zhou X, Pei C (2011) Effect of sisal fiber surface treatment on properties of sisal fiber reinforced polylactide composites. *Int J Polym Sci* 2011. <https://doi.org/10.1155/2011/803428>
60. Chaitanya S, Singh I (2017) Sisal fiber-reinforced green composites: effect of ecofriendly fiber treatment. *Polym Polym Compos* 39:4310–4321. <https://doi.org/10.1002/pc.24511>
61. Lee JT, Kim MW, Song YS et al (2010) Mechanical properties of denim fabric reinforced poly(lactic acid). *Fibers Polym* 11:60–66. <https://doi.org/10.1007/s12221-010-0060-6>
62. Graupner N, Herrmann AS, Müssig J (2009) Natural and man-made cellulose fibre-reinforced poly(lactic acid) (PLA) composites: an overview about mechanical characteristics and application areas. *Compos Part A Appl Sci Manuf* 40:810–821. <https://doi.org/10.1016/j.compositesa.2009.04.003>
63. Oksman K, Skrifvars M, Selin JF (2003) Natural fibres as reinforcement in polylactic acid (PLA) composites. *Compos Sci Technol* 63:1317–1324. [https://doi.org/10.1016/S0266-3538\(03\)00103-9](https://doi.org/10.1016/S0266-3538(03)00103-9)
64. Huang X, Netravali A (2007) Characterization of flax fiber reinforced soy protein resin based green composites modified with nano-clay particles. *Compos Sci Technol* 67:2005–2014. <https://doi.org/10.1016/j.compscitech.2007.01.007>
65. Li Y, Mai Y, Ye L (2000) Sisal fibre and its composites: a review of recent developments IM PA US AS DO ME US EX ON AS. *Compos Sci Technol* 60:2037–2055
66. Rajesh G, Ratna Prasad AV, Gupta A (2015) Mechanical and degradation properties of successive alkali treated completely biodegradable sisal fiber reinforced poly lactic acid composites. *J Reinf Plast Compos* 34:951–961. <https://doi.org/10.1177/0731684415584784>
67. Majhi SK, Nayak SK, Mohanty S, Unnikrishnan L (2010) Mechanical and fracture behavior of banana fiber reinforced polylactic acid biocomposites. *Int J Plast Technol* 14:57–75. <https://doi.org/10.1007/s12588-010-0010-6>
68. Al-Mobarak T, Mina MF, Gafur MA (2019) Material properties of sponge-gourd fiber-reinforced polylactic acid biocomposites: effect of fiber weight ratio, chemical treatment, and treatment concentrations. *J Thermoplast Compos Mater* 32:967–994. <https://doi.org/10.1177/0892705718772880>
69. Yu T, Li Y, Ren J (2009) Preparation and properties of short natural fiber reinforced poly(lactic acid) composites. *Trans Nonferrous Met Soc China (English Ed)* 19. [https://doi.org/10.1016/S1003-6326\(10\)60126-4](https://doi.org/10.1016/S1003-6326(10)60126-4)
70. Ochi S (2006) Development of high strength biodegradable composites using Manila hemp fiber and starch-based biodegradable resin. *Compos Part A Appl Sci Manuf* 37:1879–1883. <https://doi.org/10.1016/j.compositesa.2005.12.019>
71. Ochi S (2008) Mechanical properties of kenaf fibers and kenaf/PLA composites. *Mech Mater* 40:446–452. <https://doi.org/10.1016/j.mechmat.2007.10.006>
72. Sykacek E, Hrabalova M, Frech H, Mundigler N (2009) Extrusion of five biopolymers reinforced with increasing wood flour concentration on a production machine, injection moulding and mechanical performance. *Compos Part A Appl Sci Manuf* 40:1272–1282. <https://doi.org/10.1016/j.compositesa.2009.05.023>
73. Bax B, Müssig J (2008) Impact and tensile properties of PLA/Cordenka and PLA/flax composites. *Compos Sci Technol* 68:1601–1607. <https://doi.org/10.1016/j.compscitech.2008.01.004>
74. Bledzki AK, Jaszkiwicz A (2010) Mechanical performance of biocomposites based on PLA and PHBV reinforced with natural fibres - a comparative study to pp. *Compos Sci Technol* 70:1687–1696. <https://doi.org/10.1016/j.compscitech.2010.06.005>
75. Ferede E, Atalie D (2022) Mechanical and water absorption characteristics of sisal fiber reinforced polypropylene composite. *J Nat Fibers* 00:1–14. <https://doi.org/10.1080/15440478.2022.2069188>
76. Sahu P, Gupta MK (2022) Water absorption behavior of cellulosic fibres polymer composites: a review on its effects and remedies. *J Ind Text* 51:7480S–7512S. <https://doi.org/10.1177/1528083720974424>
77. Thakur VK, Singha AS (2010) Physico-chemical and mechanical characterization of natural fibre reinforced polymer composites. *Polym J* 19:3–16
78. Büyükkaya K, Demirel H (2020) Examining the mechanical and thermomechanical properties of polymethylmethacrylate composites reinforced with nettle fibres. *Arab J Sci Eng* 45:665–674. <https://doi.org/10.1007/s13369-019-04136-7>
79. Zhang Y, Yu C, Chu PK et al (2012) Mechanical and thermal properties of basalt fiber reinforced poly(butylene succinate) composites. *Mater Chem Phys* 133:845–849. <https://doi.org/10.1016/j.matchemphys.2012.01.105>
80. Vercher J, Fombuena V, Diaz A, Soriano M (2020) Influence of fibre and matrix characteristics on properties and durability of wood–plastic composites in outdoor applications. *J Thermoplast Compos Mater* 33:477–500. <https://doi.org/10.1177/0892705718807956>
81. Wang L, Feng J, He C (2022) Degradation behavior of soybean straw reinforced PLA composites in different soil conditions. *J Adhes Sci Technol* 0:1–15. <https://doi.org/10.1080/01694243.2022.2107867>
82. Kumar R, Yakubu MK, Anandjiwala RD (2010) Biodegradation of flax fiber reinforced poly lactic acid. *Express Polym Lett* 4:423–430. <https://doi.org/10.3144/expresspolymlett.2010.53>
83. Gunti R, Prasad AVR, Gupta AVSSKS (2016) Preparation and properties of successive alkali treated completely biodegradable short jute fiber-reinforced PLA composites. *Polym Compos* 37:2160–2170. <https://doi.org/10.1002/pc.23395>

**Publisher's note** Springer Nature remains neutral with regard to jurisdictional claims in published maps and institutional affiliations.

Springer Nature or its licensor (e.g. a society or other partner) holds exclusive rights to this article under a publishing agreement with the author(s) or other rightsholder(s); author self-archiving of the accepted manuscript version of this article is solely governed by the terms of such publishing agreement and applicable law.